Are your MRI contrast agents cost-effective?
Learn more about generic Gadolinium-Based Contrast Agents.
FRESENIUS KABI
caring for life

AJNR

Magnetic Resonance Imaging of the Spinal Cord and Canal: Potentials and Limitations

David Norman, Catherine M. Mills, Michael Brant-Zawadzki, Andrew Yeates, Lawrence E. Crooks and Leon Kaufman

AJNR Am J Neuroradiol 1984, 5 (1) 9-14
http://www.ajnr.org/content/5/1/9

This information is current as of April 17, 2024.

Magnetic Resonance Imaging of the Spinal Cord and Canal: Potentials and Limitations

David Norman[1]
Catherine M. Mills
Michael Brant-Zawadzki
Andrew Yeates
Lawrence E. Crooks
Leon Kaufman

Preliminary experience with magnetic resonance imaging (MRI) of the spinal cord and canal in 17 patients indicates considerable promise in the diagnosis of neoplastic, degenerative, and congenital lesions. The ability to image the cord directly rather than indirectly as in myelography, the absence of bone artifact as in computed tomography, and the multiplanar capabilities indicate that MRI will be the procedure of choice in the examination of the spinal cord. Current limitations include partial-volume effects due to slice thickness and the inability to perform contiguous sections when using multiplanar techniques. The relative increase in signal from cerebrospinal fluid with long TR and TE sequences in spin-echo imaging may result in less sensitivity than in the brain for detection of cord edema and/or infarction.

The ability of magnetic resonance imaging (MRI) to image the brain with greater sensitivity and possibly greater specificity than computed tomography (CT) [1–3] can be applied to imaging of the spinal cord and canal as well. Studies of the cord with conventional clinical techniques have achieved only limited success. The dense bony envelope limits the capabilities of x-ray CT. The cord's comparatively small size and less accessible, more variable vascular supply have limited the capabilities of angiography. Myelography has been the most successful means of imaging the cord, but provides only an indirect assessment based on visualization of the negative shadow of margins of the cord rather than the cord itself.

Our early experience with MRI in imaging the cord and its environment has been encouraging in that MRI can directly display both the normal and pathologic cord. There are, however, inherent limitations in MRI and the current equipment for this application. We discuss the possibility for resolution of these limitations in expanding applications of MRI to cord imaging.

Subjects and Methods

During the past 12 months, we have examined 17 patients with disease involving the spinal cord or spine. Four patients had pathologically confirmed neoplasms: recurrent ependymoma, teratoma, astrocytoma, and locally invasive histiocytoma, and one had renal cell carcinoma metastatic to T10 with compression of the adjacent cord. Six patients had syringomyelia (five reported previously) [4]. Two patients had tethered cords, both with associated lipomeningocele. Four patients were evaluated for disk disease, three lumbar and one cervical. All patients examined for tumor, syrinx, or cervical disk had both myelography and high-resolution computed tomography (GE CT/T 8800). Patients studied for lumbar disk disease had only CT. All lesions were confirmed surgically. Additional experience with the appearance of the normal cord was extracted from over 70 thoracoabdominal examinations performed for a variety of other disease processes.

MRI examinations were performed on a 0.35 T imager developed at the UCSF Radiologic Imaging Laboratory and undergoing constant modification during the 12-month period. The unit is capable of performing inversion-recovery and spin-echo imaging sequences, with a wide range of scan parameters available for the spin-echo technique. Spin-echo parameters

This article appears in the December 1983 issue of *AJR* and the January/February 1984 issue of *AJNR*.

Received July 19, 1983; accepted after revision August 25, 1983.

Presented in part at the annual meeting of the American Roentgen Ray Society, Atlanta, April 1983.

[1] All authors: Department of Radiology, University of California School of Medicine, San Francisco, CA 94143. Address reprint requests to D. Norman.

***AJNR* 5:9–14, January/February 1984**
0195–6108/84/0501–0009 $00.00
© American Roentgen Ray Society

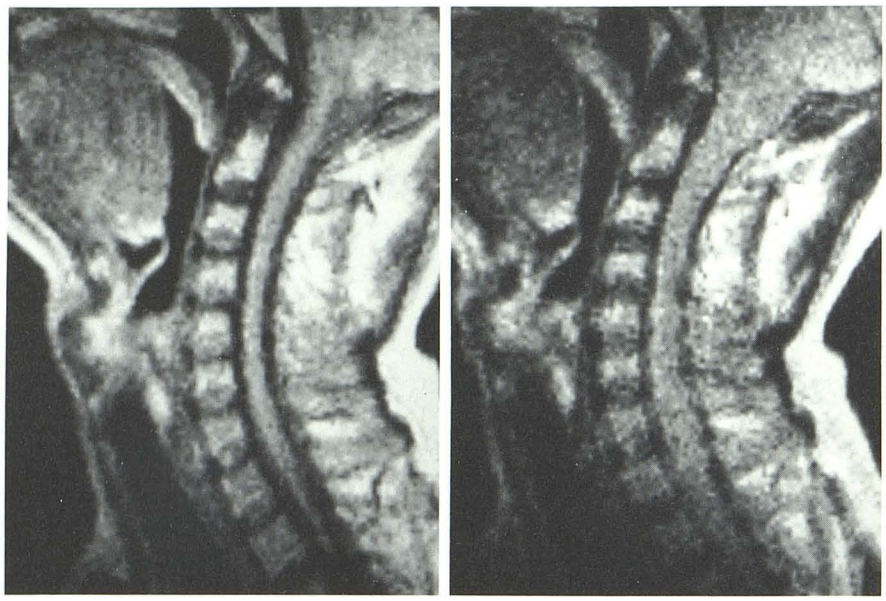

A B

Fig. 1.—Normal cervical spine, sagittal spin-echo scans. **A**, 28 msec TE, 1.5 sec TR. **B**, 56 msec TE, 1.5 sec TR. Loss of discrimination between cord and adjacent CSF space due to increased signal from CSF.

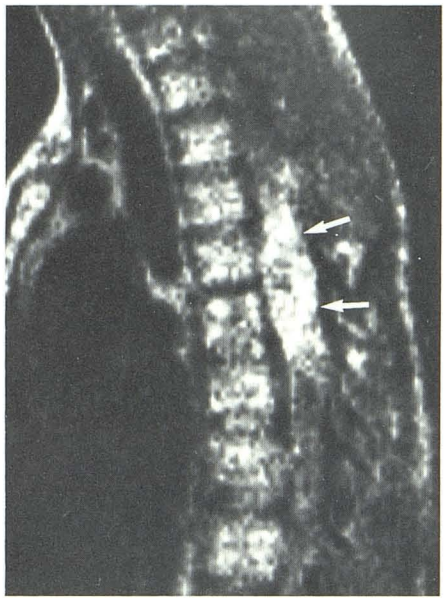

Fig. 2.—Teratoma of thoracic cord. Sagittal spin-echo scan. Lesion (*arrows*) is heterogeneous in intensity.

included a repetition time (TR) of 0.5–2 sec and an echo time (TE) of 28 and 56 msec. Initial experience suggests that the spin-echo technique is a more efficient approach to imaging and perhaps is more sensitive to the presence of pathology [5].

Imaging times were influenced to a substantial degree by the signal-to-noise (S/N) ratio desired and by the amount of quantitative data desired from the image. Anatomic images of good quality could be collected with five consecutive sections obtained in a single plane in 4.3 min. A more complete "fast scan" uses 1.5 sec TR and 28 and 56 msec TE. Fifteen sections are obtained in 6.5–13 min depending on whether two or four averages are used, the latter yielding an improved S/N ratio [6]. Since two different echoes are recorded in one sequence, a total of 30 images, two for each section, are displayed. Slice thickness is 7 mm with a 4 mm skipped area between the adjacent edges due to current electronics design. Imaging a second or third plane required an additional 6.5–17 min for each plane desired. Images are displayed with automatic scaling in which the most intense and least intense signals are used to define the upper and lower ends of the gray scale. Absolute intensity of the signal can be obtained by placing a cursor over an area of interest. No neck radiofrequency (RF) coil was available during the study, so the quality of the neck images was somewhat limited by the geometry of the body RF coil.

Although T1 and T2 data can be generated, they were not used in this study, as the absolute value is inaccurate and the relative value(s) can be determined by visual inspection of the multiple echo images [7].

Observations

MRI images with short TR and TE provided good to excellent anatomic delineation of cord morphology (fig. 1). Axial sections provided good cross-sectional representation of cord diameter; however, gray and white matter were not reliably distinguished. Sagittal imaging was performed in most patients as well. Partial-volume artifact, however, impaired the quality of the data on the longitudinal views, since averaging with adjacent cerebrospinal fluid (CSF) and/or bone provided false intensity values. Slice thickness of 7 mm and the skipped areas between slices account for the problem in the sagittal and coronal planes. Image quality and detail were related to a significant degree to imaging time, the signal improving with longer TR.

The two primary neoplasms appeared as areas of high signal intensity in comparison to the surrounding CSF, bone, and adjacent cord on the short-TR images. The recurrent ependymoma had a prolonged T2 as evidenced by increased signal on the second echo with longer TR [7]. It was imaged along its entire longitudinal axis in the sagittal plane and provided the radiotherapist with excellent anatomic landmarks. A thoracic teratoma had mixed high- and low-intensity signals indicating heterogeneous lesion, the high intensity on the short-TR, first-echo images reflecting a short T1 compatible with fat (fig. 2). At surgery, an extradural lipoma as well as the intramedullary teratoma were identified. Lipomeningoceles also had areas of high signal intensity due to the short T1 of the fatty tissue. Infiltration of a lumbar vertebra by a fibrous histiocytoma (fig. 3) appeared as an area of intensity similar to marrow on the first echo (28 msec TE, 1.5 sec TR) and increased intensity on the second echo (56 msec TE). It was also identified on CT. Infiltration of the T10 vertebral body by metastatic renal cell carcinoma with secondary canal compromise was easily seen. In this case, the high intensity from fat within the marrow was displaced by tumor of lesser

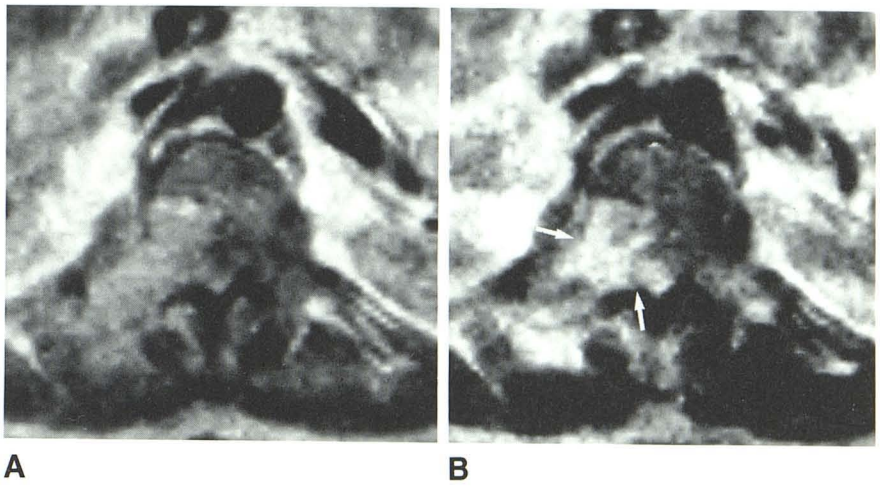

Fig. 3.—Fibrous histiocytoma infiltrating L2 vertebral body. **A**, 28 msec TE. **B**, 56 msec TE. In this sequence with relatively long TR (1.5 sec), lesion is nearly isointense with marrow on first echo (**A**) and of increased intensity on second echo (**B**) (*arrows*).

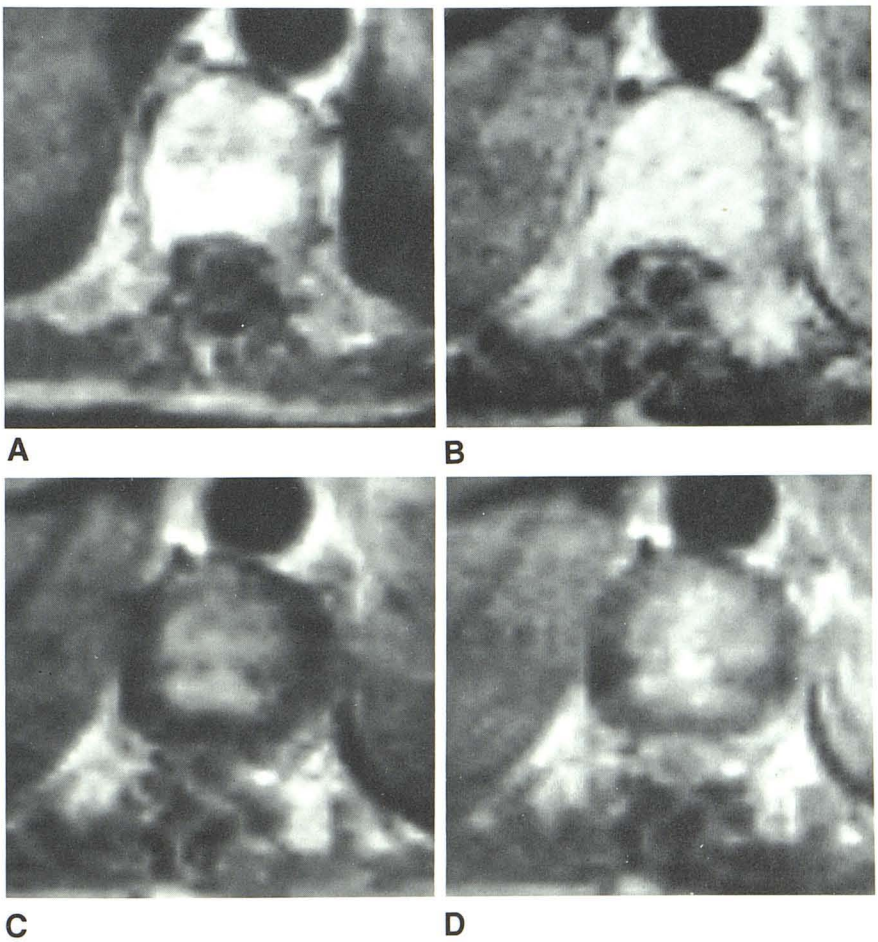

Fig. 4.—Syringomyelia. Axial images of same level at 28 msec TE and 0.5 (**A**), 1.0 (**B**), 1.5 (**C**), and 2.0 (**D**) sec TR. Longer TR results in augmentation of signal from CSF, resulting in decreased discrimination between cord and syrinx. If fluid in syrinx or subarachnoid space had elevated protein, intensity would be higher even with short TR.

signal intensity. The scan was obtained with a shorter TR (0.5 sec), which emphasized the influence of T1 on the resultant image.

The syrinxes were identified as cavities of low signal intensity in all six patients on the first echo (28 msec TE) with 0.5–2.0 sec TR. The second echo (56 msec TE) and longer TR parameter resulted in a relatively higher signal intensity from CSF compared with the cord, resulting in less contrast discrimination between the cord and the cavity as well as the surrounding CSF space (fig. 4).

In the three patients with herniated lumbar disk, the protrusion was identified but the image noise was considerably

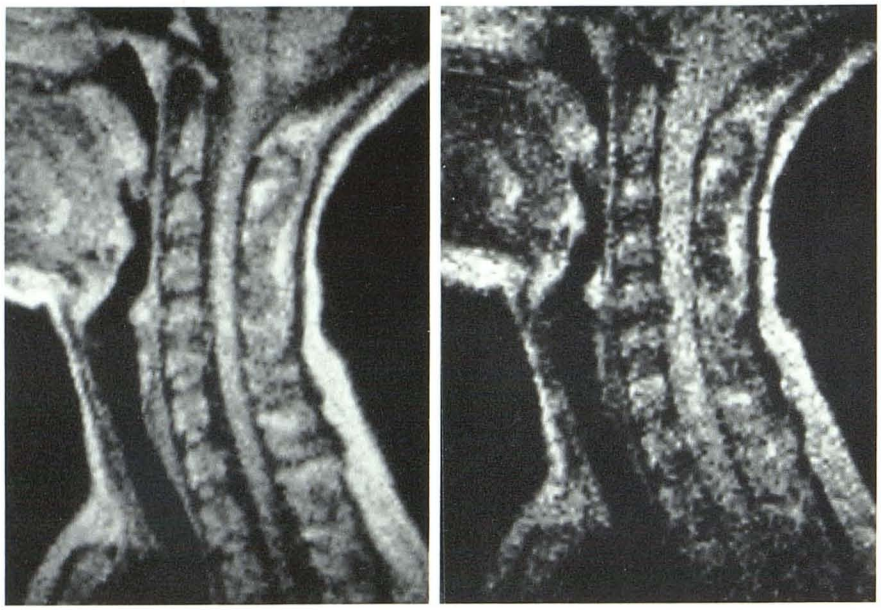

A B

Fig. 5.—C5–C6 herniated disk, sagittal spin-echo scans at 1.5 sec TR. **A**, 28 msec TE, first echo. Disk compromises subarachnoid space and abuts cord. **B**, 56 msec TE, second echo. Loss of discrimination between CSF and adjacent cord due to increased signal from CSF because of its long T2.

greater than that available with high-resolution CT. By comparison, the protruding cervical disk was well seen, best identified in the sagittal plane (fig. 4). It was detected more easily than on CT and/or myelography, despite the relatively low S/N ratio.

Discussion

Although modest in number, these initial experiences with MRI of the normal and pathologic cord illustrate the present advantages of the technique as well as some problems in methodology, information display, and accuracy.

MRI permits direct visualization of the cord and its size and shape. There is no limitation of spatial and contrast detail from signal scatter associated with adjacent bone, as encountered with x-ray CT. Thick sections and skipped areas between adjacent bone inherent in the multisection technique, however, cause partial-volume artifact, which can limit the quality and accuracy of the information.

The appearance of both the normal and pathologic cord varies with both the imaging sequence and the method of image display. Images with short TR and TE provided excellent representation of cystic cavities and of normal cord and widening due to tumor and cystic cavities; however, because there is no signal from cortical bone, the size of the CSF space may be overestimated due to lack of signal from both CSF and bone [5]. In addition, techniques using a long TR and TE result in increased signal from CSF due to T2 effect, which diminishes the ability to identify the true anatomic limits of the cord (fig. 5).

Thus far in imaging the cord, reliable gray/white differentiation has not been possible using any imaging sequence. Because of this, MRI may prove to be less sensitive in the spinal cord than in the brain in the detection of ischemic, demyelinating, or edematous lesions. Imaging sequences that are primarily T1-weighted and have high S/N ratio, such as partial saturation, may prove to be a very desirable sequence for imaging the cord (fig. 6).

Our experience with intrinsic cord tumors is too limited to make any statements concerning histologic specificity. The technique does seem to be sensitive. It is certainly superior to CT in identifying abnormal tissues or cavities; it can identify fat as readily as CT, and because of the multiplanar capabilities, it can provide superior anatomic delineation. The ability to visualize the cord directly rather than in silhouette, as in myelography, suggests that MRI may displace myelography for the diagnosis of cord neoplasms. Optimization of cord MRI will require attention to the fact that a very small part of the volume being imaged is, in fact, the area of interest. Thus target imaging techniques in which the imager is focused by means of gradient and RF coil manipulation and design should improve both the quality and content of information.

In syringomyelia, the fragile relation between a particular imaging sequence and pathology is exemplified in the situation where an increase in CSF protein causes an increase in signal and resulting decreased contrast between CSF and the adjacent cord. In a cystic cavity filled with protein, the abnormality may alter the image such that contrast is greatly reduced. This problem is not insurmountable. It may require that MRI units be designed to perform multiple imaging sequences and/or echoes at a single area of interest as well as multiple sections. Once the "most sensitive" technique is identified, it may then be used to obtain multiple slices and/or multiple planes.

Partial-volume effects, especially in the coronal and sagittal planes, also can alter the appearance of the image. Direct imaging of these planes will require thinner sections that are contiguous or overlap. Partial-volume effect and noncontig-

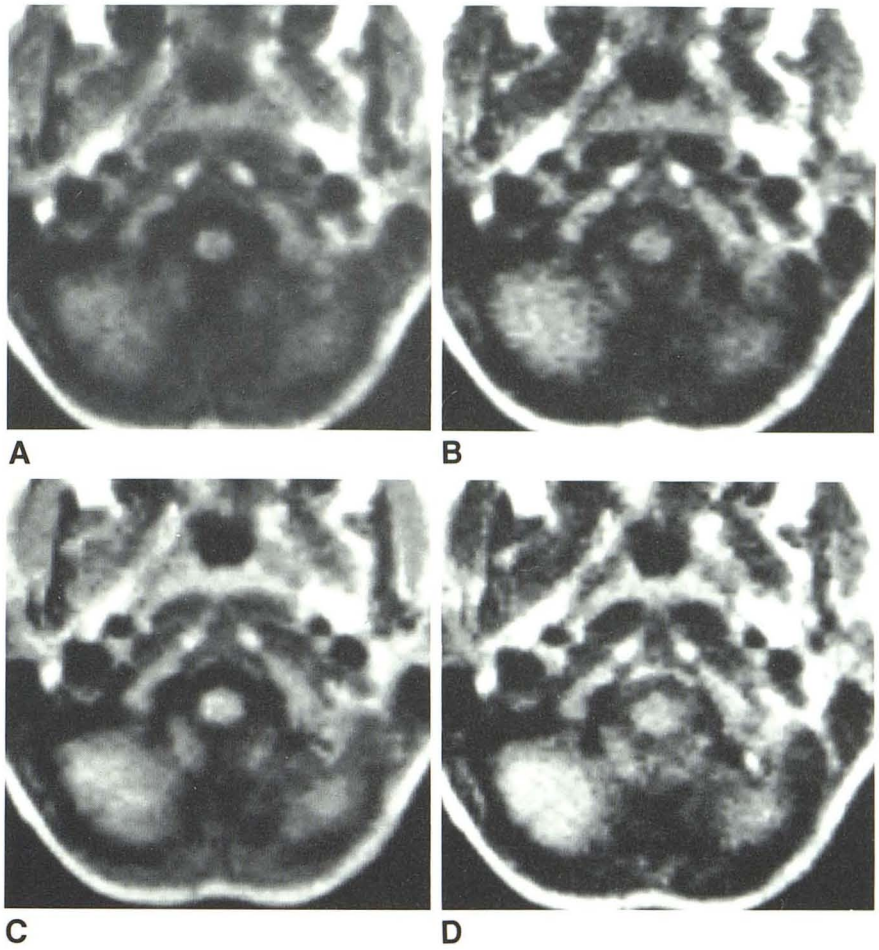

Fig. 6.—Normal cord at foramen magnum level. Spin-echo scans. **A**, 28 msec TE, 0.5 sec TR. **B**, 56 msec TE, 0.5 sec TR. **C**, 28 msec TE, 1.0 sec TR. **D**, 56 msec TE, 1.0 sec TR. Images with short TR and TE clearly demonstrate sharp distinction between cord and CSF space and suggest contrast between cord and gray/white matter. On second echo with 0.5 sec TR (**B**), gray/white matter discrimination is lost, and apparent cord diameter increases due to increase in signal from adjacent CSF. Latter phenomenon is more pronounced on **C** and **D** (longer TR). Partial-volume effects from inferior aspect of cerebellar tonsils are more pronounced with longer TR and TE.

uous sections are also limiting factors in imaging the disk space.

The low signal obtained from cortical bone, due to its relatively low mobile hydrogen content, suggests the possibility that bony lesions may be missed (e.g., a bone fragment within the canal, a sclerotic metastasis, or spinal stenosis); however, the low signal from bone is a component of the contrast and therefore is useful. A bone fragment in the canal will be seen as an area of very low signal silhouetted by the higher signal of CSF in images with a long TR and TE. Tumor invasion of bone will appear as displacement of the high signal from marrow in the cancellous bone by a signal of altered, usually diminished intensity, especially in short-TR imaging sequences. The intense signal from marrow serves to distinguish medullary from cortical bone [9]. It presumably reflects both blood and fat within the marrow.

MRI offers a unique opportunity to view anatomic, pathologic, and physiologic changes in the cord. Disease processes identified only indirectly by myelography or not appreciated at all can now be imaged in vivo. It should be possible to distinguish between intra- and extramedullary lesions, depending on the technique used. Localization of radiation treatment ports will be far more accurate than in the past.

Future applications intrinsic to MRI include taking advantage of its sensitivity to blood flow [10–13], which should permit identification of vascular malformations. It may identify the degree of ischemic compromise from these malformations and assess the result of interventional occlusive procedures. An additional area of potential application is in imaging and quantifying CSF dynamics, a subject of intense investigation for which we have relatively limited tools. Although not as yet demonstrated, the possibility of a paramagnetic agent secreted by the choroid plexus may permit both quantitative and qualitative noninvasive imaging of CSF dynamics without ionizing radiation.

REFERENCES

1. Brant-Zawadzki M, Davis PL, Crooks LE, et al. NMR demonstration of cerebral abnormalities: comparison with CT. *AJNR* **1983**;4:117–124, *AJR* **1983**;140:847–854
2. Lukes SA, Crooks LE, Aminoff MJ, et al. Nuclear magnetic imaging in multiple sclerosis. *Ann Neurol* **1983**;13:592–601
3. Bydder GM, Steiner RE, Young IR, et al. Clinical *NMR* imaging of the brain: 140 cases. *AJR* **1982**;139:215–236, *AJNR* **1982**;3:459–480
4. Yeates A, Brant-Zawadzki M, Norman D, Kaufman L, Crooks

LE, Newton TH. Nuclear magnetic resonance imaging of syringomyelia. *AJNR* **1983**;4:234–237

5. Crooks LE, Mills CM, Davis PL, et al. Visualization of cerebral and vascular abnormalities by NMR imaging: the effects of imaging parameters on contrast. *Radiology* **1982**;144:843–852
6. Crooks LE, Ortendahl DA, Kaufman L, et al. Clinical efficiency of nuclear magnetic resonance imaging. *Radiology* **1983**;146:123–128
7. Mills CM, Crooks LE, Kaufman L, Brant-Zawadzki M. Calculated T_1 and T_2 images: utility in cerebral abnormalities. *Radiology* (in press)
8. Young IR, Bailes DR, Burl M, et al. Initial clinical evaluation of a whole body nuclear magnetic resonance (NMR) tomograph. *J Comput Assist Tomogr* **1982**;6:1–18
9. Moon KL Jr, Genant HK, Helms CA, Chafetz NI, Crooks LE, Kaufman L. Musculoskeletal applications of nuclear magnetic resonance. *Radiology* **1983**;147:161–171
10. Mills CM, Brant-Zawadzki M, Crooks LE, et al. Nuclear magnetic resonance: principles of blood flow imaging. *AJNR* **1983**;4:1161–1166, *AJR* **1984**;142 (in press)
11. Kaufman L, Crooks LE, Sheldon P, et al. The potential impact of nuclear magnetic resonance imaging on cardiovascular diagnosis. *Circulation* **1983**;67:251–257
12. Crooks LE, Sheldon P, Kaufman L, Rowan W. Quantification of obstructions in vessels by nuclear magnetic resonance (NMR). *IEEE Trans Nucl Sci* **1982**;NS-29:1181–1185
13. Alfidi RJ, Haaga JR, El Yousef SJ, et al. Preliminary experimental results in humans and animals with a superconducting, whole-body, nuclear magnetic resonance scanner. *Radiology* **1982**;143:175–181